SMALL-SIGNAL MODEL EXTRACTION TECHNIQUE DEDICATED TO NOISE BEHAVIOUR OF MICROWAVE HBTs

J.G. TARTARIN, L. ESCOTTE, J. GRAFFEUIL

LAAS-CNRS and Université Paul Sabatier
7 av. du Colonel Roche, 31077 Toulouse Cedex 4, France
E-mail : tartarin@laas.fr, phone : 33.05.61.33.69.22, fax : 33.05.61.33.69.69

ABSTRACT

A complete on-wafer heterojunction bipolar transistors (HBTs) equivalent circuit parameters extraction technique is presented. It is based on the successive extraction of extrinsic and intrinsic elements. An improved method for parasitic inductance values determination is proposed. It results in a more accurate modelling of HBTs which is shown to be very useful especially for high frequency noise parameter modelling.

INTRODUCTION

An accurate heterojunction bipolar transistor small-signal equivalent circuit is needed for the design of HBTs microwave and millimeter-wave circuits. Moreover important data having a strong impact on frequency performance (access resistances, transit times in the emitter, base and collector regions...) can be obtained from such a small-signal equivalent circuit in order to assess the technological process. A physical-based equivalent circuit is also a prerequisite to analyse the noise mechanisms in the HBT. It finally must be pointed out that the more the operating frequency is high, the more the equivalent circuit complexity is high, owing to parasitics, and the more the extraction has to be accurate.

Different HBT's small-signal equivalent circuit extraction techniques have been proposed during last years [1-5] based on direct parameter extraction or using specific test structures. We propose in this paper a direct parameter extraction technique combined with an analytical method to determine the HBT's small-signal equivalent circuit. Physical-based noise sources are then embedded in this equivalent circuit resulting in a very accurate simulation of the noise performance of the device.

PARAMETER EXTRACTION TECHNIQUE

The small-signal equivalent circuit of the HBT in a common emitter configuration is depicted in figure 1. A 'T'-like topology has been retained for the intrinsic transistor representation, which is the more appropriate for noise modelling of bipolar transistors at microwave frequency compared to the hybrid-π topology.

The successive determination technique of extrinsic and intrinsic elements as suggested for the FET case [6], is modified to fit specific HBT's bias requirements.

Parasitic capacitances related to the input and output pads, and inter electrodes coupling (C_{pbe}, C_{pbc} and C_{pce}) can be easily determined if a specific test structure is available. If not, as in present work, they are determined when the collector is DC short-circuited (V_{CE}=0) by applying various base negative bias voltages (V_{BE}=V_{BC}). In that case, the emitter-base (EB) and base-collector (BC) junctions are reverse biased and the intrinsic part of the transistor is essentially made of junction transition capacitances. The combinations of intrinsic and extrinsic capacitances are determined in the low frequency range (below 2GHz) from the variations of the imaginary parts of the Y-parameters versus bias. A fitting procedure based on a standard physical model for the intrinsic transition capacitances (expression (2)) is then used to extract the parasitic elements (figure 2), according to expression (1).

$$C_{tot}(V_{BE}) = C_T(V_{BE}) + C_p \quad (1)$$

$$C_{Tei}(V_{BE}) = \frac{C_{Tei0}(V_{BE}=0)}{\left(1-\frac{V_{BE}}{\Phi_E}\right)^{m_E}} \quad \text{and} \quad C_{Tbc}(V_{BE}) = \frac{C_{Tbc0}(V_{BE}=0)}{\left(1-\frac{V_{BE}}{\Phi_C}\right)^{m_C}} \quad (2)$$

C_{Tei} and C_{Tbc} are related to the emitter-base and the base-collector transition capacitances respectively. The diffusion voltages ϕ_E and ϕ_C, the coefficients m_E and m_C relative to the nature of the junction (abrupt or gradual) and the parasitic capacitances C_p (C_{pbe} or C_{pbc}) are optimised to fit the model to the measurements by minimising the error factor between calculated and extracted total capacitance.

The extrinsic resistances and inductances can be determined from Z-parameter expressions [7] when the device is open-circuited on the collector and when the EB junction is forward biased (V_{BE} >0) :

$$Z_{11} = (R_b + r_{bi} + r_{ei} + R_e) + j\omega(L_b + L_e) \quad (3)$$

$$Z_{12} = (r_{ei} + R_e) + j\omega L_e \quad (4)$$

$$Z_{22} = (R_c + r_{bc} + r_{ei} + R_e) + j\omega(L_c + L_e) \quad (5)$$

The real parts of Z_{11}, Z_{12} and Z_{22} are extracted at low-frequency and are plotted against the inverse of the emitter current I_E [2] as shown in figures 3 and 4. The y-axis intercepts give R_e, R_b and R_c. The inductances are determined from the variations of the imaginary parts of Z_{11}, Z_{12} and Z_{22} in a higher frequency range (above 20 GHz). Negative values of the emitter inductance L_e can be found with this technique, as shown in figure 5. Indeed the intrinsic diffusion capacitance C_{ei} of the EB junction contributes to the imaginary part of Z_{12} particularly below 20 GHz resulting in an apparent L_e different from the true L_e. From the linear dependence of the diffusion capacitances C_{ei} and $C_{D\text{-}bc}$ with bias, their contribution to Z-parameters can easily be corrected : the imaginary parts of Z-parameters are plotted versus $1/I_E$ (figure 6) and the y-axis intercepts give the inductive terms. From a close examination of the analytical expressions of Z-parameters including resistances and capacitances parasitic elements (figure 7), a corrective term homogeneous to an inductance is calculated and used to obtain the true emitter inductance that can be different from the uncorrected one by more than 100% (see Appendix I for corrected expressions of L_e, L_b and L_c). The exact determination of the inductances must take into account these two steps correction to build an accurate model of the HBT. Moreover, these corrected values provide quasi-constant intrinsic parameter variation against frequency.

The HBT's intrinsic elements (when the device is in an active bias condition) are then calculated from analytical expressions after de-embedding the extrinsic cells (see Appendix II). It must be pointed out that the different transit times involved in the base transport factor α are also determined with this technique from the determination of cut-off pulsation available from the current gain expression in common base configuration.

$$\alpha = \frac{1}{1 + j\omega/\omega_e} \frac{\alpha_0 e^{-j\omega\tau}}{1 + j\omega/\omega_b} = \frac{\alpha_0 e^{-j\omega\tau}}{1 + j\omega/\omega_\alpha} \quad (6)$$

$$\omega_\alpha = (1/\omega_e + 1/\omega_b)^{-1} \quad (7)$$

ω_e and ω_b are the cut-off pulsations due to the emitter and the base regions respectively, and τ is the transit time from the base to the collector. The different obtained intrinsic parameters are frequency independent in a large frequency range, as expected, and show correct physical behaviours versus bias. Calculated (using the commercial software MDS from Hewlett Packard) and measured S-parameters are compared for a GaInP/GaAs HBT in figure 8. An excellent agreement is observed from 0.1 to 40 GHz and for a wide bias range ($0.5\ mA < I_C < 21\ mA$).

NOISE PARAMETER DETERMINATION

Unlike the 'Π' intrinsic representation, the 'T' topology is very convenient for the insertion of physical-based noise sources in the equivalent network. Nyquist noise sources are associated with each parasitic resistance. Correlated shot noise sources are inserted at the EB and BC junctions and the previously determined α gives the correlation (expressions (8) to (10)). Therefore no additional noise fitting factor is used to predict the different noise parameter variations versus frequency from a standard linear and noise simulator.

$$\overline{i_e^2} = 2qI_E\Delta f \quad (8)$$

$$\overline{i_c^2} = 2qI_C\Delta f \quad (9)$$

$$\overline{i_e^* i_c} = \frac{\alpha_0 e^{-j\omega\tau}}{1 + j\omega/\omega_b} \overline{i_e^2} \quad (10)$$

Noise parameter measurements (minimum noise figure F_{min}, equivalent noise resistance R_n and optimum reflection coefficient Γ_{opt}) have been performed with an automated test set from 1 to 18 GHz. The noise parameters calculated with our model are compared to experimental data in figure 9. A good agreement is observed which substantiates simultaneously the proposed equivalent circuit, the different parameters extraction technique and the high frequency noise sources implementation and derivation. Moreover, noise parameter variations of F_{min} and Γ_{opt} versus bias are reported in figure 10 and 11 which presents classical known behaviours.

CONCLUSION

An accurate on-wafer HBT's small signal model extraction technique has been developed. Particular care has been brought to parasitic inductances determination and an appropriate technique has been proposed to circumvent serious trouble on the emitter inductance extraction brought by the EB capacitance. Excellent agreement has been obtained between the model and the measurements. This technique has also been validated by adjunction of thermal and correlated shot noise sources in the determined equivalent circuit and noise parameter prediction from a standard linear simulator has been achieved. The observed excellent agreement with measured noise data substantiates the proposed technique and shows that any noise parameter measurement is unnecessary for HBT's as soon as an accurate equivalent network is available.

The authors would like to grateful THOMSON LCR and S.L. Delage for providing the components of this study.

REFERENCES

[1] R.J. Trew, U.K. Mishra, W.L. Pribble, J.F. Jensen, *"A parameter extraction technique for heterojunction bipolar transistors ", IEEE MTT-S symp. Dig., Long Beach, pp. 897-900, June 13-15, 1989.*

[2] S.A. Maas, D. Tait, *"Parameter extraction method for heterojunction bipolar transistor", Microwave and guided waves letters, Vol. 2, N°. 12, pp. 502-504, December 1992.*

[3] D.R. Pehlke, D. Pavlidis, *"Evaluation of the factors determining HBT high-frequency performance by direct analysis of S-parameter data", IEEE trans. MTT, Vol. 40, N°. 12, pp. 2367-2373, December 1992.*

[4] C.J Wei, J.C.M. Hwang, *"Direct extraction of equivalent circuit parameters of heterojunction bipolar transistors", IEEE trans. MTT, vol. 43, pp. 2035-2040, September 1995.*

[5] U. Schaper, B. Holzapfl, *"Analytical parameter extraction of the HBT equivalent circuit with T-like topology from measured S-parameter data", IEEE trans. MTT, Vol. 43, pp. 493-498, March 1995.*

[6] G. Dambrine, A. Cappy, F. Heliodore, E. Playez, *"A new method for determining the FET small-signal equivalent circuit", IEEE trans. MTT, Vol. 36, N°. 7, pp. 1151-1159, July 1988.*

[7] J.M. Belquin, A. Tachafine, S. Delage, A. Cappy and G. Dambrine, *"Determination of the equivalent circuit of heterojunction bipolar transistors using a full analytical method", Asia Pacific Microwave Conference 1994, pp. 603-605.*

APPENDIX I : Determination of parasitic inductances

The parasitic inductances are determined when the device is open-circuited on the collector and when the EB junction is forwarded biased ($V_{BE}>0$) [4]. In that case and assuming that $1/I_E \to 0$ (figure 6), the equivalent circuit is represented in figure 7. Z-parameters are then given by :

$$Z_{11} = j\omega\left(L_b + L_e\right) + \Delta_{11} \quad (11)$$

$$Z_{12} = Z_{21} = j\omega L_e + \Delta_{12} \quad (12)$$

$$Z_{22} = j\omega\left(L_c + L_e\right) + \Delta_{22} \quad (13)$$

where Δ_{11}, Δ_{12} et Δ_{22} are corrective terms due to R-C networks :

$$\Delta_{11} = \frac{R_b + R_e + j\omega C_{22}\left(R_e\left[R_b + R_c\right] + R_b R_c\right)}{D} \quad (14)$$

$$\Delta_{12} = \frac{R_e + j\omega C_{12}\left(R_e\left[R_b + R_c\right] + R_b R_c\right)}{D} \quad (15)$$

$$\Delta_{22} = \frac{R_c + R_e + j\omega C_{11}\left(R_e\left[R_b + R_c\right] + R_b R_c\right)}{D} \quad (16)$$

with :

$$D = 1 - \omega^2\left(C_{11}C_{22} - C_{12}^2\right)\left(R_e\left[R_b + R_c\right] + R_b R_c\right) + j\omega\left(R_e\left[C_{11} + C_{22} - 2C_{12}\right] + R_b C_{11} + R_c C_{22}\right) \quad (17)$$

$$C_{11} = C_{pbe} + C_{pbc} \quad (18)$$

$$C_{12} = C_{pbc} \quad (19)$$

$$C_{22} = C_{pce} + C_{pbc} \quad (20)$$

The development of expressions 14 to 16 (neglecting ω^2, ω^4...) leads to the following expressions of the imaginary parts of Δ_{11}, Δ_{12} and Δ_{22} :

$$\mathrm{Im}\{\Delta_{11}\} \approx \left[-(R_b+R_e)^2 C_{11} + 2R_e(R_b+R_e)C_{12} - R_e^2 C_{22}\right]\omega \tag{21}$$

$$\mathrm{Im}\{\Delta_{12}\} \approx \left[-R_e(R_b+R_e)C_{11} + \left(R_e^2 + (R_b+R_e)(R_c+R_e)\right)C_{12} - R_e(R_c+R_e)C_{22}\right]\omega \tag{22}$$

$$\mathrm{Im}\{\Delta_{22}\} \approx \left[-R_e^2 C_{11} + 2R_e(R_c+R_e)C_{12} - (R_c+R_e)^2 C_{22}\right]\omega \tag{23}$$

The parasitic inductances are then given by :

$$L_b = \left(\mathrm{Im}\{Z_{11}-Z_{12}\} - \mathrm{Im}\{\Delta_{11}-\Delta_{12}\}\right)/\omega \tag{24}$$

$$L_e = \left(\mathrm{Im}\{Z_{12}\} - \mathrm{Im}\{\Delta_{12}\}\right)/\omega \tag{25}$$

$$L_c = \left(\mathrm{Im}\{Z_{22}-Z_{12}\} - \mathrm{Im}\{\Delta_{22}-\Delta_{12}\}\right)/\omega \tag{26}$$

APPENDIX II : Determination of intrinsic parameters

The base transport α factor is given by the following expression :

$$\alpha = \frac{Z_{12}-Z_{21}}{Z_{22}-Z_{21}} \tag{27}$$

where Z_{ij} are the intrinsic parameters of the transistor.
α_0 is determined from the modulus of α at low frequency. ω_α and τ are given by :

$$\omega_\alpha = \frac{\omega}{\sqrt{\left(\frac{\alpha_0}{|\alpha|}\right)^2 - 1}} \tag{28}$$

$$\tau = -\frac{phase(\alpha) + Artg\left(\omega/\omega_\alpha\right)}{\omega} \tag{29}$$

The other intrinsic parameters are given by :

$$r_{bi} = \mathrm{Re}\{Z_{11}-Z_{12}\} \tag{30}$$

$$r_{ei} = \frac{1}{\mathrm{Re}\{1/Z_{12}\}} \tag{31}$$

$$C_{ei} = \frac{\mathrm{Im}\{1/Z_{12}\}}{\omega} \tag{32}$$

The emitter cut-off pulsation ω_e is calculated from equations (31) and (32), and the base cut-off pulsation ω_b is then deduced from :

$$\omega_e = \frac{1}{r_{ei}C_{ei}} \quad \text{and} \quad \omega_b = \left(1/\omega_\alpha - 1/\omega_e\right)^{-1} \tag{33}$$

$$r_{bc} = \frac{1}{\mathrm{Re}\left\{\frac{1}{Z_{22}-Z_{21}}\right\}} \tag{34}$$

$$C_{bc} = \frac{\mathrm{Im}\left\{\frac{1}{Z_{22}-Z_{21}}\right\}}{\omega} \tag{35}$$

FIGURES CAPTION

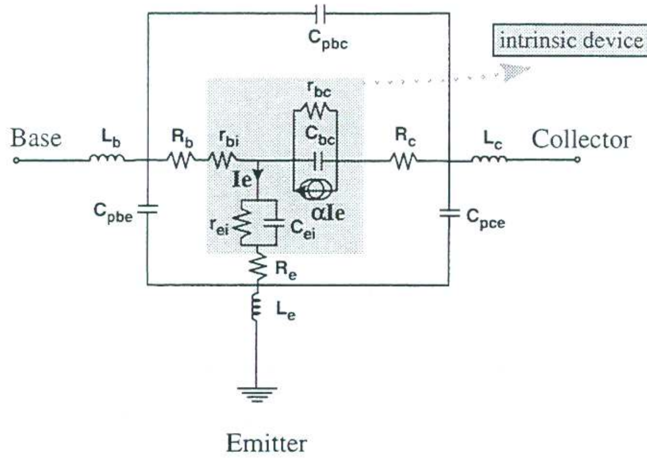

Fig. 1 : HBT's small-signal equivalent circuit

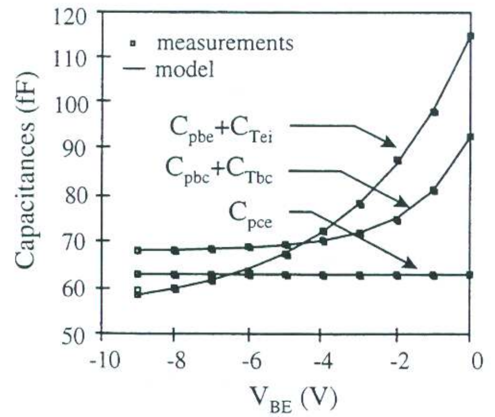

Fig. 2 : determination of parasitic capacitances

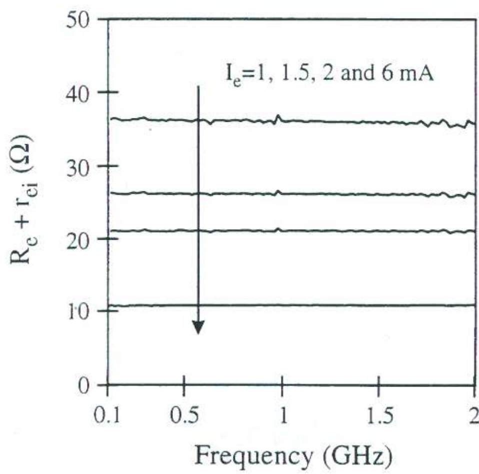

Fig. 3 : Emitter resistance variations versus frequency for different bias conditions

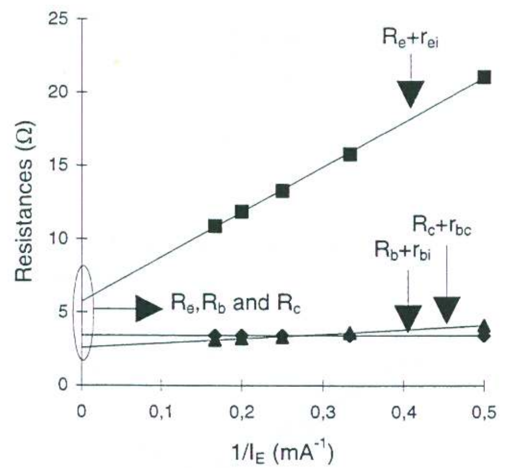

Fig. 4 : resistances variations versus $1/I_E$

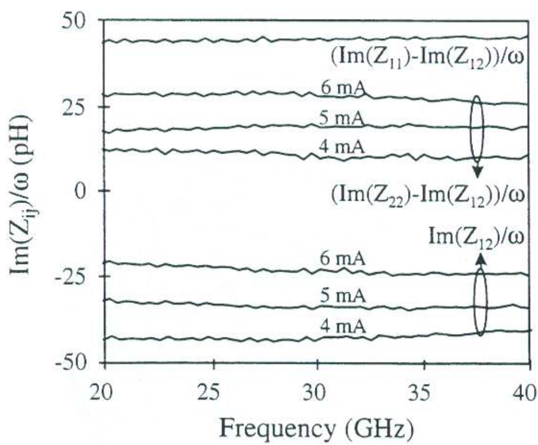

Fig. 5 : inductance variations versus frequency for different bias conditions.

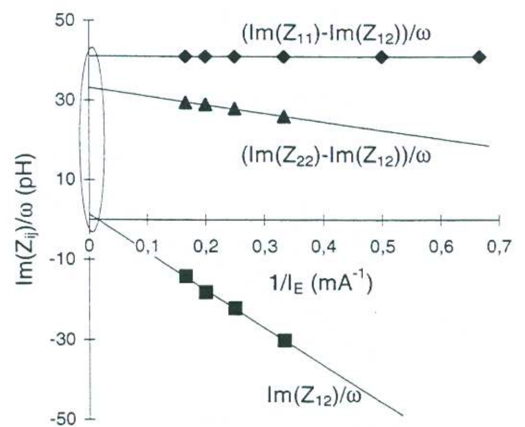

Fig. 6 : inductance variations versus $1/I_E$

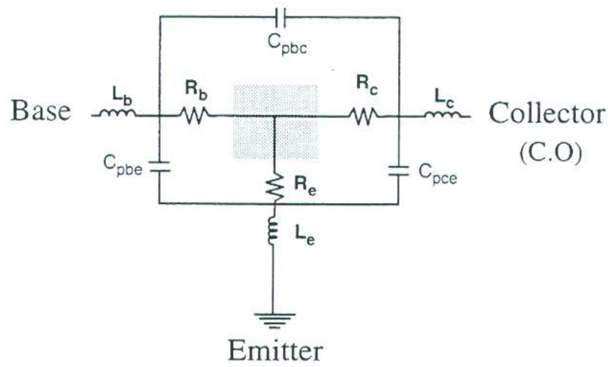

Fig. 7 : HBT's equivalent circuit with EB junction forward biased (V_{BE}>0), with $1/I_E \rightarrow 0$

Fig. 8 : Comparison between calculated (—) and measured (+) S-parameters from 0.1 to 40 GHz for a GaInP/GaAs HBT featuring $2x30\mu m^2$ emitter surface, at V_{CE}=2V, I_C=21mA.

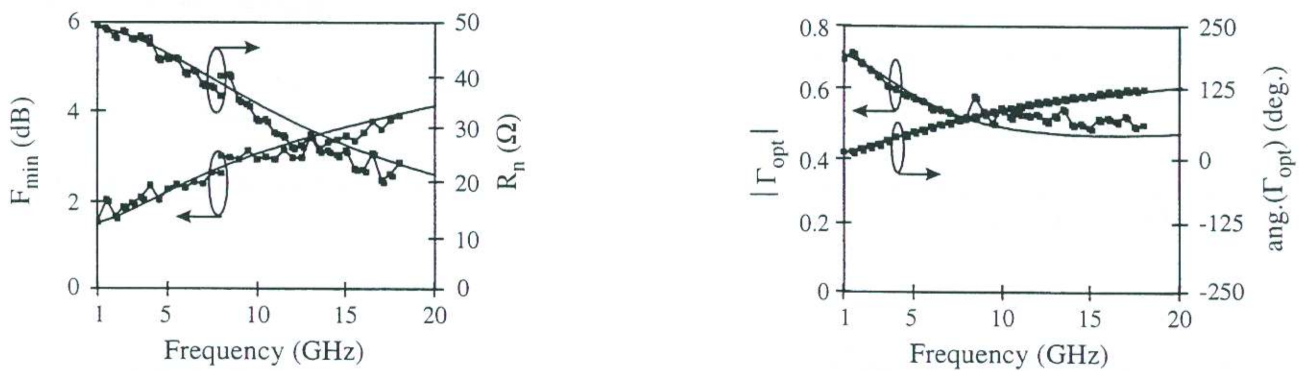

Fig. 9 : noise parameters versus frequency for a GaInP/GaAs HBT biased at I_C=0.5mA and V_{CE}=2V (— : model, ■ : measurement)

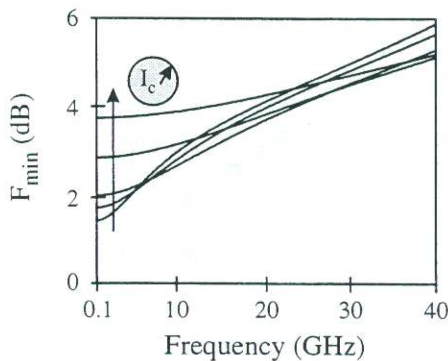

Fig. 10 : minimum noise figure versus frequency for $I_C \in$ (0.5, 1, 2, 5, 10 mA) (– model)

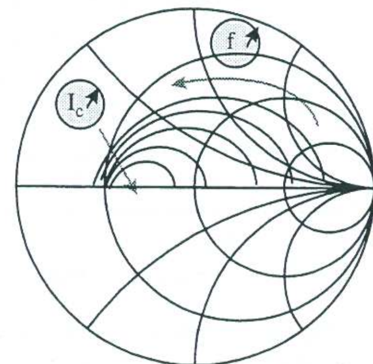

Fig. 11 : optimum reflection coefficient Γ_{opt} for $I_C \in$ (0.5, 1, 2, 5, 10 mA) from 0.1 to 40 GHz